Cretaceous Research 79 (2017) 159–170

Contents lists available at ScienceDirect

Cretaceous Research

journal homepage: www.elsevier.com/locate/CretRes

Multiple paleopathologies in the dinosaur *Bonitasaura salgadoi* (Sauropoda: Titanosauria) from the Upper Cretaceous of Patagonia, Argentina

Romina Gonzalez [a, *], Pablo A. Gallina [b], Ignacio A. Cerda [c]

[a] *Centro de Ecología Aplicada del Litoral (CECOAL-CONICET), C.P. 3400, Corrientes, Argentina*

[b] *Área de Paleontología, Fundación Félix de Azara, Universidad Maimonides, CONICET, Hidalgo 775, C1405BCK Buenos Aires, Argentina*

[c] *Universidad Nacional de Río Negro, CONICET, Instituto de Investigaciones en Paleobiología y Geología, Museo Provincial "Carlos Ameghino", Belgrano 1700, Paraje Pichi Ruca (predio Marabunta), CP8300 Cipolletti, Río Negro, Argentina*

ARTICLE INFO

Article history:
Received 17 January 2017
Received in revised form
15 July 2017
Accepted in revised form 20 July 2017
Available online 22 July 2017

Keywords:
Osseous abnormalities
Titanosaurs
Paleobiology
South America

ABSTRACT

Bones in the fossil record sometimes exhibit unusual structures that can be attributed to pathologies, taphonomic alterations, or morphological variation. The goal of this work is to describe three bone abnormalities present in the type specimen of *Bonitasaura salgadoi* from the Cretaceous of north Patagonia, Argentina. The studied material corresponds to a left femur, a left metatarsal III, and a right prezygapophysis of a mid-caudal vertebra. Macroscopic and/or histological examinations were conducted, and a discussion concerning the origin of each abnormality is provided. The results of this study suggest that the anomalous structures are pathologies. In the femur, an osteoblastic tumor was identified by the presence of a large outgrowth of ovoid appearance with a spiculated microstructural pattern. The metatarsal III shows an enthesophyte (or bone spur) based on its location, shape and growth in parallel to the long axis of the bone element. Finally, the abnormal tissue observed in the prezygapophysis of the caudal vertebra was determined to be an infection by the presence of reactive new bone associated with a local widening of the subperiosteal margin and a sinus of drainage. This is the first report of multiple pathologies in a single specimen of a titanosaur, and it provides new insights about paleopathologies in sauropod dinosaurs.

1. Introduction

Vertebrates have a complex skeletal system that is susceptible to disease and trauma. Diseases and traumas usually leave distinct traces on bones that, allow for the identification of different types of pathologies in living and extinct organisms (e.g., Rothschild and Martin, 2006; Rothschild, 2009). Paleopathology is the study of ancient disease and injuries (trauma) in the fossil to subfossil record (Tanke and Rothschild, 2002). Paleopathological studies provide information about the paleobiology, including lifestyle and behavior, of extinct groups (e.g., Hanna, 2002; Ferigolo, 2007; Martinelli et al., 2015).

Osseous pathologies in non-avian dinosaurs have been well documented in both saurischian and ornithischian taxa and include: fractures (e.g., Sullivan et al., 2000; Straight et al., 2009; Xing et al., 2009; Hedrick et al., 2016), infections (e.g., Hanna, 2002; McWhinney et al., 2001b; Bell and Coria, 2013; Cerda et al., 2014; Redelstorff et al., 2015; Anné et al., 2016; García et al., 2016), osteopetrosis (e.g., Chinsamy and Tumarkin-Deratzian, 2009), degenerative disorders (e.g., Tanke and Rothschild, 2014), tumors (e.g., Rothschild et al., 1998; Rothschild et al., 1999; de Souza Barbosa et al., 2016; Dumbravă et al., 2016) and developmental disorders (Witzmann et al., 2008). In the case of sauropodomorph dinosaurs, paleopathological studies have been conducted in taxa such as *Apatosaurus* Marsh 1877 (Gilmore, 1936; Rothschild and Berman, 1991; Reid, 1996); *Camarasaurus* Cope 1877 (McWhinney et al., 2001a; Tschopp et al., 2016); *Diplodocus* Marsh 1878 (Hatcher, 1901; Rothschild, 1987; Rothschild and Berman, 1991); and *Uberabatitan ribeiroi* Salgado and Carvalho 2008 (Martinelli et al., 2015). This last case corresponds to a titanosaur species that was described as having two fused vertebrae and a hemal arch with a fracture callus in two specimens. The fused vertebrae were

* Corresponding author. Centro de Ecología Aplicada del Litoral CONICET, Ruta 5, km 5,2, C.P. 3400, Corrientes, Argentina.
E-mail address: romigonzl95@gmail.com (R. Gonzalez).

http://dx.doi.org/10.1016/j.cretres.2017.07.013

interpreted as the result of a spondyloarthropathy, an infection, or both (Martinelli et al., 2015).

Additionally, three reports on indeterminate titanosaurs have been published (Chinsamy et al., 2016; de Souza Barbosa et al., 2016; García et al., 2016). Chinsamy et al. (2016) reported on the occurrence of three unusual bone tissues located in different skeletal elements (metatarsal, vertebra and osteoderm) within an indeterminate saltasaurine from the Upper Cretaceous of Argentina. In this case, the unusual histology of the metatarsal was only diagnosed as a pathological response. de Souza Barbosa et al. (2016) mentioned two types of bone tumors (hemangioma and osteoma) in a caudal vertebra corresponding to a titanosaur from Brazil. Finally, García et al. (2016) reported evidence of osteomyelitis in a caudal vertebra from a titanosaur from the Upper Cretaceous of Argentina. In addition to these particular studies, Gallina (2012) and Gallina and Apesteguía (2015) reported osseous abnormalities from femur, metatarsal III and prezygapophysis in the holotype of *Bonitasaura salgadoi* Apesteguía 2004 (Upper Cretaceous of Patagonia, Argentina), which were tentatively interpreted as possible pathologies. However, a detailed analysis of these skeletal abnormalities was not performed.

The specific goal of this work is to describe the abnormalities mentioned in the femur, metatarsal III and prezygapophysis from type specimen of *B. salgadoi*. Additionally, the possible causes and paleobiological significance of these abnormalities are discussed. We provide an analysis of the abnormalities through macroscopic and histological examinations. The three abnormalities analyzed are related to osseous paleopathologies. This is the first report of multiple pathologies in a single specimen of a titanosaur, and thus, it provides new insights about paleopathologies in sauropod dinosaurs.

2. Materials and methods

All the postcranial skeletal elements from the holotype of *B. salgadoi* (MPCA 460) were macroscopically examined. Since osseous abnormalities where found only in three bones (left femur, left metatarsal III, and a right prezygapophysis of a mid-caudal vertebra), this study focused on these elements. The sauropod titanosaur *B. salgadoi* was collected in the Bajo de la Carpa Formation (Santonian), Río Negro province, northern Patagonia, Argentina (Apesteguía, 2004; Gallina and Apesteguía, 2011, 2015) (Fig. 1). The materials were deposited in the collection of the Museo Provincial Carlos Ameghino (MPCA), Cipolletti, Río Negro province, Argentina.

Three types of analyses were performed: 1) an examination of the gross morphology (femur and metatarsal), 2) a histologic examination (femur and prezygapophysis), and 3) a CT scan (metatarsal). For the macroscopic evaluation of osseous pathologies, we followed Rega (2012). In this regard, we considered the texture, shape, type of bone response (proliferative, lytic or mixed), longitudinal location (epiphyseal, metaphyseal or diaphyseal) and its transverse location (medullary, cortical or juxtacortical). We used the term "outgrowth" (exostosis) to refer to the abnormal bone that grew from the bone surface, as defined by Cohen et al. (1973).

The materials were analyzed using both visual inspection and an Olympus (SZ51) stereoscope microscope. Images were taken with a Panasonic (DMC-S5) camera. Histological sections where obtained from the normal and abnormal areas of the femur. The gross morphology of the prezygapophysis of the caudal vertebra could not be assessed because thin sections had previously been made by Gallina (2012) and pictures of the element where not taken before sectioning. Thin sections of the femur were prepared at the Laboratorio de Petrografía of the Instituto de Geocronología y Geología Isotópica (INGEIS) of the Universidad de Buenos Aires (UBA), according to the method outlined by Chinsamy and Raath (1992). The bone histological terminology follows Francillon-Vieillot et al. (1990) and de Ricqlès et al. (1991). The thin sections were studied using a Zeiss Axioskop 40 petrographic polarizing microscope, with an attached PowerShot A640 digital camera (Canon). The metatarsal III was scanned on a Siemens Somatom Emotion 16 multislice CT at the Departamento de Radiología of the Fundación Médica Cipolletti, Río Negro Province. Due to both the size and the weight of the element, a CT scan analysis of the femur could not be performed.

3. Results

3.1. Femur

This element exhibits a focal bony outgrowth, located on the posterior side, below the fourth trochanter, approximately 33 cm

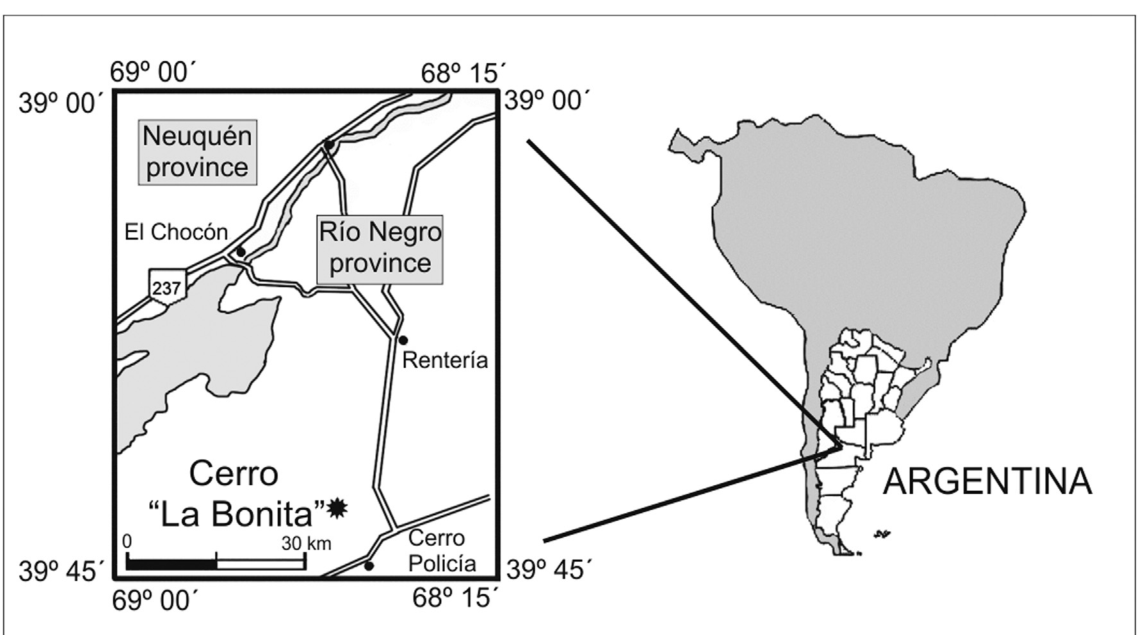

Fig. 1. Map of "La Bonita" site, Río Negro province, Argentina where the holotype (MPCA 460) of *Bonitasaura salgadoi* was found (taken from Gallina and Apesteguía, 2011).

Fig. 2. Macroscopic examination of the left femur (MPCA 460) of *B. salgadoi*. (A) Posterior view exhibiting bony outgrowth (dashed line), below of the fourth trochanter (4th tr); (B) Detail of the abnormality in posterior view. Note the irregular surface and superficial depressions (black arrow) in the mid-half anterior of the outgrowth. Dashed line indicates planes of natural break observed at Fig. 2D and 2E; (C) Femur in lateral view showing a dense bony mass (outgrowth). The black arrow indicates a natural break on the bone; (D) General view and detail of a natural fracture across the outgrowth (transverse to the element main axis). Note the presence of large vascular spaces radially oriented; (E) General view of a natural fracture of the outgrowth (longitudinal to the element main axis). Note the spiculated pattern of the vascular spaces. Scale bars: A–C = 10 cm; D = 2 cm; E = 1 cm. White arrow indicate the end proximal in B–C and external surface in D–E.

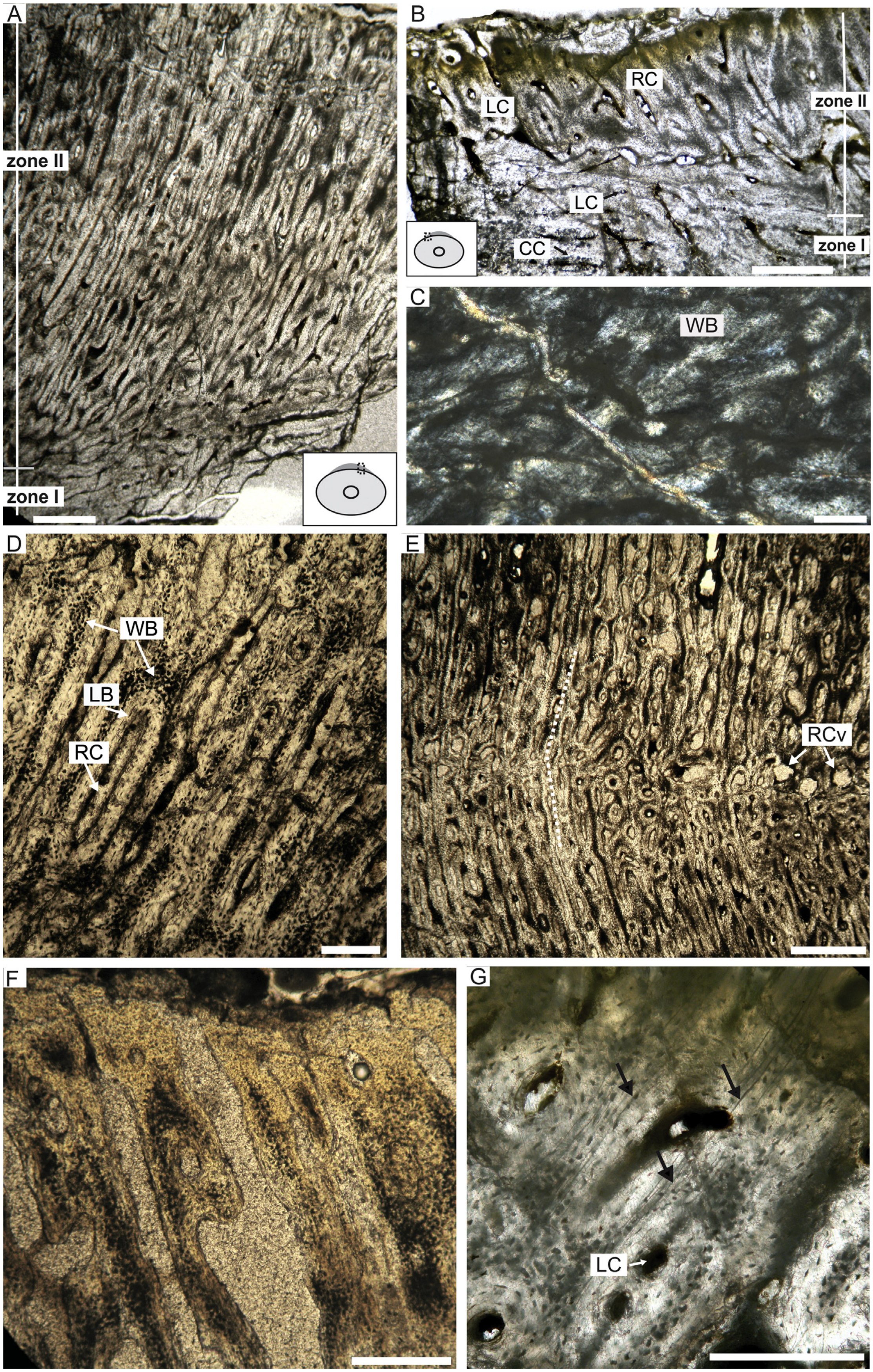
A
zone II
zone I
B
RC
LC
zone II
LC
CC
zone I
C
WB
D
WB
LB
RC
E
RCv
F
G
LC

from the distal end (femur length equal to 118.5 cm) (Fig. 2A). The outgrowth has a well-defined margin, and it is clearly distinctive from the surrounding normal bone. The bony outgrowth shows an oval shape, and its dimensions are approximately 21 cm in proximo-distal length and 11.6 cm in latero-medial width. The surface of the outgrowth varies from roughly smooth (in the distal region) to irregular (in the proximal region). The irregular portion exhibits superficial depressions that disrupt the bone surface (Fig. 2B). In lateral and medial views, the outgrowth protrudes up to 4.5 cm from the normal surface of the shaft (Fig. 2C). Natural fractures occurring at the level of the abnormality allowed for a gross examination of the internal anatomy of this bone. The outgrowth is internally highly porous, and it exhibits some relatively larger spaces (maximum diameter: 1.15 mm) (Fig. 2D). It is not possible to determine if a similar type of abnormal bone tissue is also present within the marrow cavity. A natural, longitudinal fracture of the outgrowth reveals that the anomalous bone shows a spiculated pattern. These spiculae are perpendicular to the long axis of the femur (Fig. 2E).

The thin section shows two well-defined tissues: the outer cortex of bone (zone I) and an anomalous tissue (zone II). The transition between the two zones is abrupt and well defined (Fig. 3A–B). Zone I consists of a highly vascularized fibrolamellar tissue, with circumferentially and longitudinally oriented channels, embedded in a woven bone matrix (Fig. 3C). The osteocyte lacunae are small and ovoid, showing regular length canaliculi. This periosteal cortical bone tissue was also identified by Gallina (2012) in the outer cortex of a cross section of the femur, which was obtained from a "normal" (i.e., lacking anomalous outgrowth) portion of the element. Zone II exhibits fibrolamellar tissue with mostly radially oriented vascular channels (Fig. 3D). Longitudinal channels are also present. In some cases, radial rows of elongated primary osteons are discernible. The diameter of these channels varies from 0.16 mm to 0.04 mm. Osteocyte lacunae from primary osteons are flattened and oriented in parallel to the lamellae. Short canaliculi radiate from these lacunae. The woven fibered bone of the matrix contains densely packed globular osteocyte lacunae which exhibit long canaliculi. A striking feature of zone II is the change in the orientation of the vascularization (Fig. 3E). This inclination of the channels generates an obtuse angle of approximately 160°. Although some resorption cavities are clearly identified, no secondary osteons are observed in zone II. Towards the periphery of the sample, bone spiculae and vascular channels open to the surface (Fig. 3F). Sharpey's fibers, oriented perpendicular to the external surface, were also identified (Fig. 3G).

3.2. Metatarsal III

This element displays an osseous outgrowth (spur-like) on the medial face of the element, in the region of about the proximal third of the diaphysis (Fig. 4A). The abnormal spur-like structure exhibits a wide base that contacts the shaft. The outgrowth reaches a proximo-distal length of 3 cm, is roughly parallel to the long axis of the element, and is distinct from the surrounding bone. The osseous outgrowth is an asymmetrical structure that exhibits a roughly triangular shape. The proximal end of the outgrowth shows two projections, one with a laminar shape and the other with subcircular shape (Fig. 4B). The distal end of the outgrowth shows another small bony projection with a circular shape (Fig. 4C). The abnormal spur-like structure, exhibits a slightly roughened texture (Fig. 4D). Tomographic images reveal that there is not any particular alteration (i.e., presence of reactive endosteal bone) in the marrow cavity at level of the superficial outgrowth (Fig. 4E–F).

3.3. Middle caudal vertebra

The osseous abnormality is only observed in the subperiosteal margin of the prezygapophysis of the vertebra (Fig. 5A). Underlying this tissue there is Haversian bone, which represents the normal tissue, as reported by Gallina (2012). The zone of transition between the Haversian tissue and the abnormal tissue is gradual and, without a clear boundary. The abnormal tissue corresponds to a reactive new bone with a dome shape, and it exhibits a distinct cavity/canal filled with sedimentary matrix. The border of the cavity is composed of fibrolamellar tissue, resulting in a pitted surface (Fig. 5B). The abnormal bone tissue consists of poorly vascularized fibrolamellar tissue (Fig. 5C). The primary osteons lack spatial organization and consist of a few longitudinal vascular canals (max. diameter: 0.2 mm) that, occur in a woven bone matrix composed of bundles of coarse mineralized fibers (Fig. 5D). Moreover, abundant and densely grouped osteocyte lacunae are visible in the woven matrix. In the adjacent region to the Haversian tissue, a few small resorption cavities are developed (Fig. 5E). Sharpey's fibers were not observed in the area corresponding to the abnormal tissue.

4. Discussion

4.1. Origin of the abnormal structures

The abnormal osseous structures recognized in the three bones of the holotype of *B. salgadoi* could be the result of distinct causes, including taphonomic alterations, normal (nonpathologic) morphological variation of the bones or pathological deformities. Taphonomic processes affect bones, mainly by eroding (through insect boring, root marks, chemical dissolution, transport, etc.) and/or deforming (by compression, mineral or sediment adhesion, etc.) the osseous structure (Wilson, 1988; Bell, 1990; Lyman, 1994). However, these alterations are absent in the studied material. Perez et al. (2009) carried out a stratigraphic and taphonomical analysis of the *B. salgadoi* remains and concluded that the individual was rapidly buried after death (low transport), allowing for (along with other taphonomic causes) the excellent preservation of this specimen. Additionally, the bone tissue of the abnormal osseous structures does not exhibit signals of taphonomic alteration. Another possible explanation for the presence of osseous outgrowths in the femur and metatarsal and the subperiosteal excavations in the prezygapophysis could be related to a normal anatomical variation of the skeleton that can be related to the development of the associated soft tissues (Witmer, 1997; Tsuihiji, 2004; O'Connor, 2006; Holliday, 2009). In the case of the metatarsal III, the osseous outgrowth observed in this element is absent in the other preserved metatarsals (left: I, II and V; right: I, II, IV and V) of the same specimen. Moreover, such structure is not reported in the metatarsal III of other sauropod dinosaurs (e.g., Curry Rogers, 2009; González Riga et al., 2016). The dome-shaped structure observed in

Fig. 3. Bone microstructure of the left femur (MPCA 460) of *B. salgadoi.* (A and B) General view of the cross-section showing transition between the anomalous tissue (zone II) and normal bone (zone I). The inset scheme of each image indicates the locations of the transverse section; (C) Normal primary bone composed of fibrolamellar bone tissue with woven bone matrix; (D) Anomalous bone tissue formed by fibrolamellar bone tissue with radially oriented vascular channels; (E) General view of the anomalous tissue showing the slight change in the canals orientation (dashed line); (F) Outer cortex of the outgrowth showing several vascular canals opened into the subperiosteal surface; (G) Outer cortex of the outgrowth showing aligned Sharpey's fiber (black arrows). All pictures are in normal light except figure C (polarized light). Abbreviations: CC: circumferential canal; RC: radial canal; LC: longitudinal canal; LB: lamellar bone; WB: woven bone, RCv: resorption cavity. Scale bars: A, B, E = 0.5 mm; C, D, F, G = 0.1 mm.

Fig. 4. Morphology of the left metatarsal III (MPCA 460) of *B. salgadoi*. (A) Medial view showing a distinct outgrowth (dashed line); (B) Detail of the outgrowth in medio-ventral view. Note the two projections of laminar and subcircular shape (dashed line); (C) Ventral view showing another small projection on the surface bone (arrow); (D) Dorsal view shows slightly roughened surface; (E) Longitudinal CT scan showing the outgrowth as an extension of normal cortical bone; (F) Four axial CT slices at different positions along of the outgrowth showing a dense mineralization that not extend into the cancellous bone interior. Scale bars: A and E = 10 cm; B–C = 5 cm; D = 2 cm and F = 3 cm.

the prezygapophysis has not been recorded in other caudal vertebrae of the same specimen (RG pers. obs.). In the case of the distinct outgrowth observed in the femur, a direct comparison with the other femur is not possible since it is not preserved. Nevertheless, morphological comparisons with other titanosaurian femora reveal that such a structure is absent. A site for a strong muscular insertion can be excluded because the histological analysis does not support this interpretation, given the absence of extrinsic fibers (Petermann and Sander, 2013). The anomalous structures exhibit reactive new bone, in the subperiosteal margin of the bones, which is congruent with a pathological condition. For these reasons, and in agreement with the original interpretation of Gallina (2012) and Gallina and Apesteguía (2015), we conclude that the abnormalities present in the bones of *B. salgadoi* MPCA 460 analyzed here are the product of pathological conditions of the individual.

4.2. Identification of osseous pathology

4.2.1. Femur

The bony outgrowth detected in the femur could be the result of several types of pathologies, such as trauma (e.g., fracture), infection (e.g., avian osteopetrosis) or tumor (e.g., osteosarcoma, osteoid osteoma). Fracture is excluded here because neither internal disruption (fracture line) nor bone callus formation was observed in this element (Rothschild and Martin, 1993; Lovell, 1997; Rothschild, 1997). Avian osteopetrosis is a viral infection that causes circumferential deposition of bone around the entire diaphysis (Brothwell, 2002); however, we have observed a focal and well-defined lesion in the femur. Another possible cause could be related with a microbial infection transferred from adjacent soft tissue (Hanna, 2002). However, significant features that characterized bone infection, such as abscess formation, filigree texture, draining channel (cloacae), formation of involucrum (new bone that forms around a sequestrum) and sequestrum (dead bone) (Ortner and Putschar, 1981; Rothschild and Martin, 2006), were not observed in the femur. Finally, the relative large size, ovoid appearance and spiculated appearance of the bone tissue suggest an osteoblastic bone tumor (bone forming) for the pathology detected in the femur (Edeiken et al., 1966; Lehrer et al., 1970; Wenaden et al., 2005; Green and Mills, 2014). Neoplasms (tumor) result in uncontrolled and uncoordinated cell proliferation with extensive cortical disruption and the formation of abnormal masses (Aluja and Vanda-Cantón, 2011). In a clinical context, fresh tissue pathology is the basis for the diagnosis of bone tissue tumors (de Boer et al., 2013). Nevertheless, morphological and microanatomical features can also provide important data for the diagnosis of possible tumors in bone elements (Waldron, 2009; Rega, 2012). In addition, some tumors are more commonly formed in particular bone elements and locations, which facilitates the diagnosis (Miller, 2008). A classification of the different tumors and their main features are summarized in Table 1. A hemangioma and Erwing's sarcoma are unlikely causes because the former commonly affect vertebral bodies, and the latter is characteristically intramedullary in a transverse location (Bárbara et al., 1999; Rana et al., 2009). Osteoid osteoma and metastasis can also be excluded because osteolytic (nidus) and holes in the surface ("golf-ball surface" appearance) are not present in the femur (Rothschild et al., 1998; Rothschild and Martin, 2006). A parosteal osteosarcoma might be a possible explanation for the lesion observed in our study. Parosteal osteosarcoma is a malignant bone tumor formed at a slow growth rate (Waldron, 2009). This type of tumor can achieve very significant sizes and is predominantly localized in the posterior surface of the distal portion of the femur (Waldron, 2009). The spiculated pattern observed in the tumor tissue is similar to a "sunburst" type of periosteal reaction, which is frequently observed in an osteosarcoma (Edeiken et al., 1966; Lehrer et al., 1970; Wenaden et al., 2005; Green and Mills, 2014). In addition, the irregular texture and depressions observed in the surface of the lesion could be result of lytic bone destruction that often characterize osteosarcoma (López, 2003). However, the lesion in the femur shows a well-defined margin and a narrow transition zone, which are uncommon features in malignant tumors such as parosteal osteosarcoma. Moreover, the prevalence of abundant radial canals imbedded in a woven fibered matrix indicates fast rates of bone formation, which does not concur with a parosteal osteosarcoma hypothesis (Greenspan and Remagen, 2002). In this regard, parosteal osteosarcoma is characterized by the presence of "streamers" of trabecular bone, with intervening neoplastic spindle cell stroma (the so-called "streamer pattern") (Hang and Chen, 2014). Therefore, although the bone pathology observed in the femur of *B. salgadoi* MPCA 460 can be regarded as an osteoblastic bone tumor, its specific type cannot be discerned.

Tumors have been reported throughout the entire spectrum of vertebrates in the fossil record (Capasso, 2005). Reports about tumors in non-avian dinosaurs are relatively scarce, but they have been some reports, including: hemangioma, metastatic cancer, desmoplastic fibroma, osteoblastoma, osteoma, and ameloblastoma (Rothschild et al., 1999; Arbour and Currie, 2011; de Souza Barbosa et al., 2016; Dumbravă et al., 2016; Tschopp et al., 2016). The hadrosauroids have an apparent predisposition to tumoral pathologies (Dumbravă et al., 2016). In sauropod titanosaurs, to date, only the study of de Souza Barbosa et al. (2016) reports two possible cases of benign tumors in a caudal vertebra (osteoma and hemangioma). Thus, the femur MPCA 460 is only the second record of a tumor in titanosaurs.

A particular histological feature observed in the tumoral tissue of *B. salgadoi* consists of a clear change in the orientation of the radial vascular spaces. Variations in the vascular pattern of anomalous tissues have been interpreted as evidence for biomechanically adaptive periosteal bone modeling in other non-avian dinosaurs (Cubo et al., 2015). Nevertheless, the current data do not provide evidence to support/reject this hypothesis.

4.2.2. Metatarsal III

The abnormal outgrowth detected in the metatarsal resembles two conditions: an enthesophyte (bony projection along tendon/ligament attachments) and an osteochondroma (benign neoplasms) (Greenspan and Remagen, 2002). This last case can be ruled out because the abnormal outgrowth lacks cortical and medullar continuity from the host bone, which is a pathognomonic feature of an osteochondroma (Murphey et al., 2000). Moreover, the osteochondroma presents "cauliflower-like" appearance and grows at right angles to the surface of the bone (Resnick, 2002). These features are absent in the metatarsal of *B. salgadoi*. Additionally, the features detected in the metatarsal that are congruent with the presence of an enthesophyte or bony spur include: location periarticular, asymmetrical morphology, and projection in parallel to the long axis of the bone (Benjamin et al., 2006; Campillo et al., 2006; Bell, 2010). An enthesophyte is an abnormal bony projection at the attachment of a tendon or ligament (Rogers et al., 1997). This abnormality is caused by different diseases, such as spondyloarthropathies, diffuse idiopathic skeletal hyperostosis (DISH) and repetitive stresses (Rothschild and Martin, 2006; Bell, 2010; García et al., 2016). However, DISH and spondyloarthropathy are typically reported in both the axial skeleton and joints, respectively (Rothschild and Rothschild, 1994; Resnick, 2002; Rothschild and Martin, 2006). Therefore, those diseases can be excluded for our case study. An enthesophyte, by repetitive stress on ligament or tendon, is the most likely explanation for the outgrowth in metatarsal III. This outgrowth is in parallel to the shaft of the bone, indicating the direction of the natural pull of the

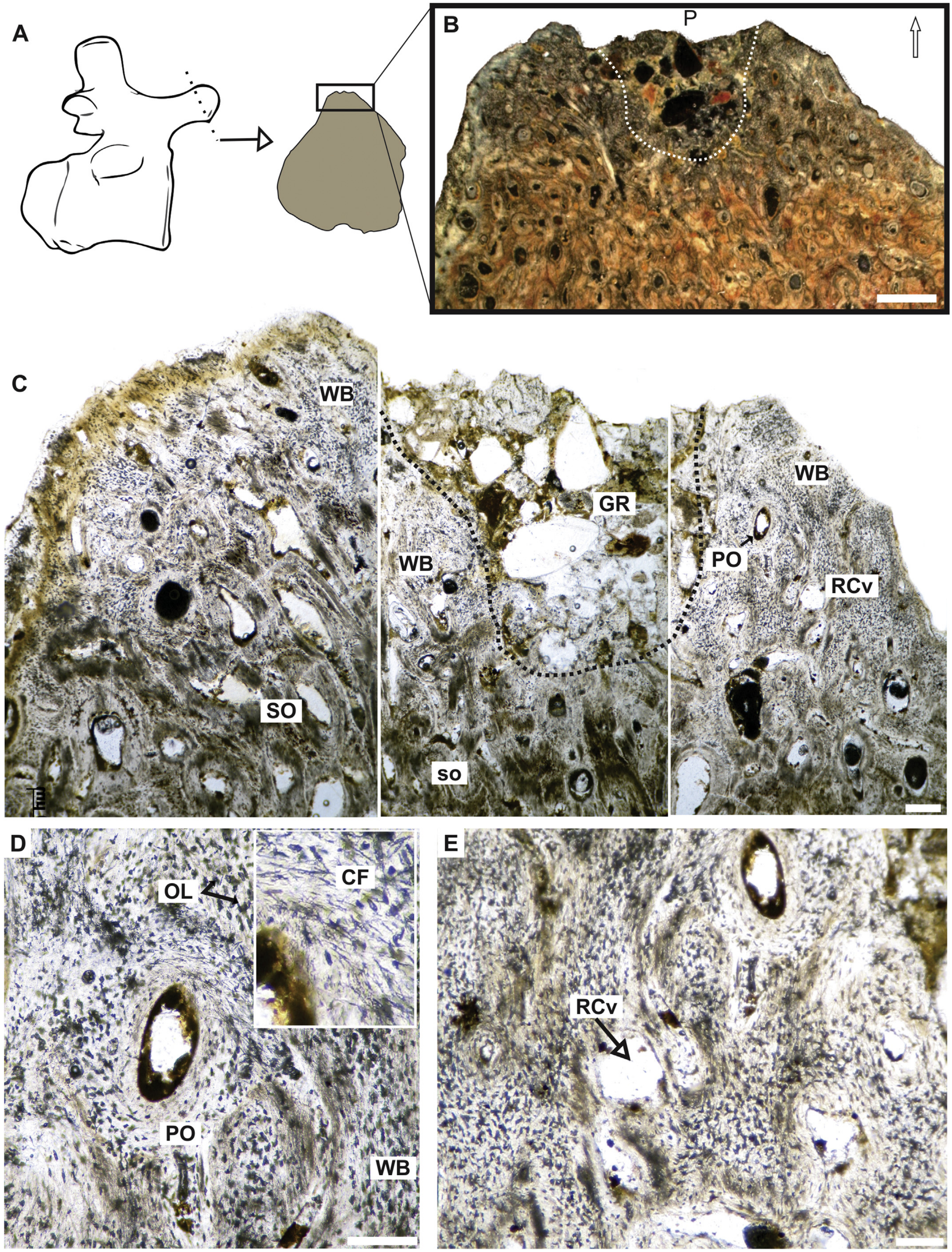
A
B
P
C
WB
GR
WB
WB
PO
RCv
SO
so
D
OL
CF
PO
WB
E
RCv

Table 1
Osseous tumors and their main features (Eggli et al., 1993; Greenspan and Remagen, 2002; Rothschild and Martin, 2006; Miller, 2008; Rana et al., 2009).

Bone tumor	Bone commonly affected	Margin definition	Type of destruction	Zone of transition	Comments
Periosteal Hemangioma	Vertebral bodies	Well defined	Lytic	Narrow	Benign vascular tumor characterized by "polka-dot" appearance in cross section.
Osteoid Osteoma	Femur, tibia (all areas of the bone)	Well defined	Sclerotic	Narrow	Benign bone tumor characterized by "button-like" appearance and the presence of a small focus lytic (nidus).
Parosteal Osteosarcoma	Femur (distal diaphyses)	Ill-defined	Sclerotic	Wide	Malignant tumor of low grade. Cortical destruction and marrow invasion is uncommon.
Erwing's sarcoma	Long bones (diaphyses and metaphyses)	Ill-defined	Lytic	Wide	Malignant tumor. There is a permeative destruction pattern with irregular cortical destruction. Intramedullary in transverse location
Metastasis	Wide skeletal distribution	Ill-defined	Lytic	Wide	Frequently form multiple holes, irregular trabeculae, and present residual cortical shell.

ligament or tendon involved (Rogers et al., 1997). The position of the lesion in the metatarsal is probably correlated with the insertion site for the muscle *extensor digitorum longus* (Tarsitano, 1981; Gallina, 2011). Therefore, the bony outgrowth of the Metatarsal III is identified as bony spur or enthesophyte.

Enthesophytes have been previously noted in non-avian dinosaurs. Farke and O'Connor (2007) reported an abnormal growth in a caudal vertebra of the theropod *Majungasaurus crenatissimus* Depéret 1896. This abnormality was attributed to an idiopathic ossification or a possible enthesophyte. Bell (2010) reported a theropod *Albertosaurus sarcophagus* Osborn 1905 with bony spurs in three pedal phalanges. These bony spurs were interpreted as enthesophytes of unknown etiological origin. Arbour and Currie (2011) reported bony spicules in caudal vertebrae of *Euoplocephalus* Lambe 1910 (ankylosaurid). The authors suggest either developmental abnormalities or enthesophytes as probable cause of the lesion. Tschopp et al. (2016) reported enthesophytes in pedal unguals of a camarasaurid sauropod. García et al. (2016) mentioned the presence of enthesophytes in two caudal vertebrae of an undetermined titanosaur. Therefore, the identification of an enthesophyte in *B. salgadoi* MPCA 460 represents the third report of this type of osseous pathology in sauropod dinosaurs.

4.3. Caudal vertebra

The abnormal tissue noted in the prezygapophysis of the caudal vertebrae is here interpreted as a periosteal bone inflammation, likely by infection. The infection is recognized by the presence of reactive new bone associated with local widening of the subperiosteal margin and sinus of drainage (Rothschild and Martin, 2006; Waldron, 2009; Rothschild, 2010; Weston, 2012). These features are recognized in the prezygapophysis of the caudal vertebra of MPCA 460. The fibrolamellar tissue is considered the reactive new bone from the subperiosteal margin, and the cavity observed in the fibrolamellar tissue is interpreted as a drainage canal of infectious material into adjacent tissues (sinus of drainage). The fibrolamellar tissue exhibits a dome shape that could be result of the elevation of the periosteum due to infection (Weston, 2012). The abundant woven bone matrix from this tissue indicates a rapid rate of osteogenesis in the affected area (Chinsamy-Turan, 2005). Bone infections occur when pathogenic organisms invade the bone, such as bacteria, viruses, parasites, etc (Weston, 2012).

Infections associated with traumatic injuries, as well as non-traumatic injuries, have been documented in several non-avian dinosaurs (e.g., McWhinney et al., 2001b; Hanna, 2002; Canudo et al., 2005; Peterson and Vittore, 2012; Bell and Coria, 2013; Redelstorff et al., 2015; Mallon et al., 2016). In titanosaur sauropods, García et al. (2016) reported a case of osteomyelitis that affected a sequence of 16 caudal vertebrae.

5. Paleobiological implications

The three pathologies are closely related to the subperiosteal margin. In living vertebrates, an organic layer of connective tissue (i.e., periosteum) is located above this margin. The periosteum is a dynamic zone composed by two layers; an outer fibrous layer and an inner cellular layer (Wenaden et al., 2005) that is osteoblastic (Allen et al., 2004) and could lead to neoplasm and other tumor-like conditions (McWhinney et al., 2001a). Many types of pathologies are caused by the inflammation of the periosteum resulting in periostitis (Meese and Sebastianelli, 1996; Wenaden et al., 2005; Rana et al., 2009). Adler (2000) mentioned that pathologies associated with the periosteum also cause pain because it is a highly sensitive layer. Therefore, the pathologies reported for *B. salgadoi* MPCA 460 are all related with periosteum and probably caused periostitis and pain to this individual.

The possible bone tumor in the femur could have affected the adjacent muscles such as the *adductors femores* group. These muscles insert on the posterior surface of the diaphysis of the femur in extant archosaurs and, by inference, reconstructed as such in titanosaurs (Borsuk-Bialynicka, 1977; Otero and Vizcaíno, 2008; Gallina, 2011). McWhinney et al. (2001a) mentioned a case of periostitis in the distal diaphysis of the humerus of *Camarasaurus grandis* Cope 1877 that, could have caused a secondary inflammation of the muscles (myositis). Therefore, a similar inflammation could be inferred in the associated musculature near the large tumor observed in the femur.

Regarding the pathology in the caudal vertebra, it is interesting to note that the infection is localized in the tail, a region of high mobility in sauropods (Borsuk-Bialynicka, 1977; Wilson and Carrano, 1999; Farke and O'Connor, 2007). In diplodocids and the derived titanosaur, the "whiplash" tail has been interpreted as a defensive function or noisemaking specialization (e.g., Hatcher, 1901; Holland, 1915; Norman, 1985; Bakker, 1986; Myhrvold and

Fig. 5. Bone histology of the prezygapophysis of mid-caudal vertebra (MPCA 460) of *B. salgadoi*. (A) Schematic representation of the vertebra (left) and an outline of prezygapophysis in cross section showing the location of the abnormal structure. Dashed line in the vertebral diagram indicates where the sample was taken; (B) General view of the abnormal tissue showing both fibrolamellar and Haversian bone. Dashed line indicates the border of cavity infilled with sediment; (C) Detail of the abnormal tissue showing extensive development of woven fibered bone, primary osteons and a cavity filled with sedimentary matrix; (D) Abnormal tissue is composed of woven matrix with densely packed osteocyte lacunae. Note the bundles of coarse mineralized fibers (detail in the upper right margin); (E) A cavity of osteoclastic resorption associated with abnormal tissue was observed. Abbreviations: P: pore; WB: woven bone; SO: secondary osteon; GR: grain of sediment; PO: primary osteon; OL: osteocyte lacunae; RCv: resorption cavity; CF: coarse mineralized fibers. Scale bars B = 1 mm; C–E = 0, 1 mm.

Currie, 1997). Therefore, the tail could be particularly susceptible to injury and subsequent infection of the overlying soft tissue.

It is also worth noting that the tumor in the femur and the enthesophyte in the metatarsal III are both located in the same limb and, therefore, could be related. Therefore, the tumor possibly affected the normal locomotion of the individual, provoking an increased stress on a tendon of the metatarsal III. This would promote the formation of the enthesophyte.

6. Conclusions

The results of these analyses suggest that the abnormal bony structures observed in the left femur, in the metatarsal III, and in the caudal vertebra of the holotype (MPCA 460) of *B. salgadoi* are the result of three different etiologies. In the femur, an osteoblastic tumor was identified by the presence of a large outgrowth of ovoid appearance and spiculated bone pattern. The origin of the tumor is unknown. The bony outgrowth identified in the metatarsal shows a case of enthesophyte based on both the location, shape and type of growth. The origin of this pathology is possibly the result of repetitive stress. Finally, the abnormal tissue observed in the prezygapophysis of the caudal vertebra is recognized as an infection by the presence of reactive new bone associated with local widening of the subperiosteal margin, and a sinus of drainage. The cause of this pathology probably is a response to an infection in the tail. We suspect that the pathologies identified would have limited the locomotor capabilities of the animal. Finally, to date, this is the first report of multiple pathologies in a single titanosaur individual. These results contribute to our knowledge of dinosaur paleopathologies and, particularly, titanosaur sauropods.

Acknowledgments

We thank Carlos Muñoz for the access to the specimens under his care in the MPCA, Cipolletti, Río Negro. Daniela Gamboa, Daniel Domínguez and the authorities of the Fundación Médica (Cipolletti) for their help with CT scans. A. Elbakyan, J. Bar and Wikipaleo group provided important useful literature. A. Martinelli and an anonymous reviewer for providing constructive criticism and suggestions that improved the original manuscript. The authors also thank Sr. Eduardo Llanbias (INGEIS-CONICET) for the preparation of the histological sections. This work has been partially funded by Agencia Nacional de Promoción Científica y Técnica (PICT 2015-1021 to I.A.C).

References

Adler, C.P., 2000. Bones and bone tissue. In: Adler, C.P., Feldman, F., Dahlin, D.C. (Eds.), Bones Diseases: Macroscopic, Histological and Radiological Diagnosis of Structural Changes in the Skeleton. Springer, Berlin, pp. 1–8.

Allen, M.R., Hock, J.M., Burr, D.B., 2004. Periosteum: biology, regulation, and response to osteoporosis therapies. Bone 35, 1003–1012. http://dx.doi.org/10.1016/j.bone.2004.07.014.

Aluja, A.S., Vanda-Cantón, B., 2011. Sistema musculoesquelético. In: Trigo, T.F.J. (Ed.), Patología sistémica, fifth ed. McGraw-Hill, Mexico, pp. 227–261.

Anné, J., Hedrick, B.P., Schein, J.P., 2016. First diagnosis of septic arthritis in a dinosaur. Royal Society Open Science 3, 160222. http://dx.doi.org/10.1098/rsos.160222.

Apesteguía, S., 2004. *Bonitasaura salgadoi* gen. et sp. nov.: a beaked sauropod from the Late Cretaceous of Patagonia. Naturwissenschaften 91, 493–497. http://dx.doi.org/10.1007/s00114-004-0560-6.

Arbour, V.M., Currie, P.J., 2011. Tail and pelvis pathologies of ankylosaurian dinosaurs. Historical Biology 23, 375–390. http://dx.doi.org/10.1080/08912963.2011.563849.

Bakker, R.T., 1986. The Dinosaur Heresies: New Theories Unlocking the Mystery of the Dinosaurs and their Extinction. William Morrow, New York, p. 480.

Bárbara, J.P., Tarazona, P.V., Zambito, G.B., 1999. Hemangioma vertebral sintomático. Anales Médicos del Hospital ABC 44, 138–140.

Bell, L.S., 1990. Palaeopathology and diagenesis: an SEM evaluation of structural changes using backscattered electron imaging. Journal of Archaeological Science 17, 85–102. http://dx.doi.org/10.1016/0305-4403(90)90016-X.

Bell, P.R., 2010. Palaeopathological changes in a population of *Albertosaurus sarcophagus* from the Upper Cretaceous Horseshoe Canyon Formation of Alberta, Canada. Canadian Journal of Earth Sciences 47, 1263–1268. http://dx.doi.org/10.1139/E10-030.

Bell, P.R., Coria, R.A., 2013. Palaeopathological survey of a population of *Mapusaurus* (Theropoda: Carcharodontosauridae) from the Late Cretaceous Huincul Formation, Argentina. PLoS One 8, e63409. http://dx.doi.org/10.1371/journal.pone.0063409.

Benjamin, M., Toumi, H., Ralphs, J.R., Bydder, G., Best, T.M., Milz, S., 2006. Where tendons and ligaments meet bone: attachment sites ('entheses') in relation to exercise and/or mechanical load. Journal of Anatomy 208, 471–490. http://dx.doi.org/10.1111/j.1469-7580.2006.00540.x.

Borsuk-Bialynicka, M., 1977. A new camarasaurid sauropod *Opisthocoelicaudia skarzynskii*, gen. n., sp. n. from the Upper Cretaceous of Mongolia. Palaeontologia Polonica 37, 1–64.

Brothwell, D., 2002. Ancient avian osteopetrosis; the current state of knowledge. Acta Zoologica Cracoviensia 45, 315–318.

Campillo, D., Devenat, L., Guixé, E.G., 2006. Problemas conceptuales de las entesopatías en paleopatología. Eres. Arqueología/Bioantropología 14, 105–120.

Canudo, J.I., Barco, J.L., Cruzado-Caballero, P., Cuenca-Bescós, G., Ruiz-Omeñaca, J.I., Royo-Torres, R., 2005. Evidencias de predación de dinosaurios terópodos en el Maastrichtiense Superior, Cretácico Superior de Arén (Huesca). Lucas Mallada 12, 29–58.

Capasso, L.L., 2005. Antiquity of cancer. International Journal of Cancer 113, 2–13. http://dx.doi.org/10.1002/ijc.20610.

Cerda, I.A., Chinsamy, A., Pol, D., 2014. Unusual endosteally formed bone tissue in a Patagonian basal sauropodomorph dinosaur. The Anathomical Record 297, 1385–1391. http://dx.doi.org/10.1002/ar.22954.

Chinsamy-Turan, A., 2005. The Microstructure of Dinosaur Bone: Deciphering Biology with Fine-Scale Techniques. Johns Hopkins University Press, Baltimore, p. 195.

Chinsamy, A., Raath, M.A., 1992. Preparation of bone histological study. Palaeontologia Africana 29, 39–44.

Chinsamy, A., Tumarkin-Deratzian, A., 2009. Pathologic bone tissues in a turkey vulture and a nonavian dinosaur: implications for interpreting endosteal bone and radial fibrolamellar bone in fossil dinosaurs. The Anatomical Record 292, 1478–1484. http://dx.doi.org/10.1002/ar.20991.

Chinsamy, A., Cerda, I.A., Powell, J., 2016. Vascularised endosteal bone tissue in armoured sauropod dinosaurs. Scientific Reports 6, 24858. http://dx.doi.org/10.1038/srep24858.

Cohen, H.J., Frank, S.B., Minkin, W., Gibbs, R.C., 1973. Subungual exostoses. Archives of Dermatology 107, 431–432.

Cope, E.D., 1877. On a gigantic saurian from the Dakota epoch of Colorado. Paleontological Bulletin 25, 5–10.

Cubo, J., Woodward, H., Wolff, E., Horner, J.R., 2015. First reported cases of biomechanically adaptive bone modeling in non-avian dinosaurs. PLoS One 10, e0131131. http://dx.doi.org/10.1371/journal. pone.0131131.

Curry Rogers, K., 2009. The postcranial osteology of *Rapetosaurus krausei* (Sauropoda: Titanosauria) from the Late Cretaceous of Madagascar. Journal of Vertebrate Paleontology 29, 1046–1086.

de Boer, H.H., Van der Merwe, A.E., Maat, G.J.R., 2013. The diagnostic value of microscopy in dry bone palaeopathology: a review. International Journal of Paleopathology 3, 113–121. http://dx.doi.org/10.1016/j.ijpp.2013.03.004.

Depéret, C., 1896. Note sur les dinosauriens sauropodes & théropodes du Crétacé supérieur de Madagascar. Bulletin de la Société Géologique de France 24, 176–194.

de Ricqlès, A., Meunier, F.J., Castanet, J., Francillon-Vieillot, H., 1991. Comparative microstructure of bone. In: Hall, B.K. (Ed.), Bone, volume 3: Bone Matrix and Bone Specific Products. CRC Press, Boca Raton, pp. 1–78.

de Souza Barbosa, F.H., da Costa, P.V.L.G., Bergqvist, L.P., Rothschild, B.M., 2016. Multiple neoplasms in a single sauropod dinosaur from the Upper Cretaceous of Brazil. Cretaceous Research 62, 13–17. http://dx.doi.org/10.1016/j.cretres.2016.01.010.

Dumbravă, M.D., Rothschild, B.M., Weishampel, D.B., Csiki-Sava, Z., Andrei, R.A., Acheson, K.A., Codrea, V.A., 2016. A dinosaurian facial deformity and the first occurrence of ameloblastoma in the fossil record. Scientific Reports, 6. http://dx.doi.org/10.1038/srep29271.

Edeiken, J., Hodes, P.J., Caplan, L.H., 1966. New bone production and periosteal reaction. American Journal of Roentgenology 97, 708–718.

Eggli, K.D., Quiogue, T., Moser Jr., R.P., 1993. Ewing's sarcoma. Radiologic Clinics of North America 31, 325–337.

Farke, A.A., O'Connor, P.M., 2007. Pathology in *Majungasaurus crenatissimus* (Theropoda: Abelisauridae) from the Late Cretaceous of Madagascar. Journal of Vertebrate Paleontology 27 (Memoir 8, 2, Supplement), 180–184. http://dx.doi.org/10.1671/0272-4634(2007)27[180:PIMCTA]2.0.CO;2.

Ferigolo, J., 2007. Paleopatologia em Mamíferos. In: Carvalho, I.S., Fernandes, A.C.S. (Eds.), Icnologia Sao Paulo, Sociedade Brasileira de Geologia. Editora Interciência, Rio de Janeiro, pp. 88–107.

Francillon-Vieillot, H., de Buffrénil, V., Castanet, J., Geraudie, J., Meunier, F.J., Sire, J.Y., Zylberberg, L., de Ricqlès, A., 1990. Microstructure and mineralization of vertebrate skeletal tissues. In: Carter, J.G. (Ed.), Skeletal Biomineralization: Patterns, Processes and Evolutionary Trends. Van Nostrand Reinhold, New York, pp. 471–548.

Gallina, P.A., 2011. Estudio anatómico, sistemático y paleobiológico de *Bonitasaura salgadoi* (Dinosauria, Sauropoda): su importancia en el contexto de la evolución de los titanosaurios del Cretácico Superior de la Argentina (Unpubl. PhD thesis). Universidad Nacional de La Plata, 340 pp.

Gallina, P.A., 2012. Histología ósea del titanosaurio *Bonitasaura salgadoi* (Dinosauria; Sauropoda) del Cretácico Superior de Patagonia. Ameghiniana 49, 289–302.

Gallina, P.A., Apesteguía, S., 2011. Cranial anatomy and phylogenetic position of the titanosaurian sauropod *Bonitasaura salgadoi*. Acta Palaeontologica Polonica 56, 45–60. http://dx.doi.org/10.4202/app.2010.0011.

Gallina, P.A., Apesteguía, S., 2015. Postcranial anatomy of *Bonitasaura salgadoi* (Sauropoda, Titanosauria) from the Late Cretaceous of Patagonia. Journal of Vertebrate Paleontology 35, 1–22. http://dx.doi.org/10.1080/02724634.2014.924957.

García, R.A., Cerda, I.A., Heller, M., Rothschild, B.M., Zurriaguz, V., 2016. The first evidence of osteomyelitis in a sauropod dinosaur. Lethaia. http://dx.doi.org/10.1111/let.12189.

Gilmore, C.W., 1936. Osteology of *Apatosaurus*, with special reference to specimens in the Carnegie Museum. Memoirs of the Carnegie Museum 11, 175–300.

González Riga, B.J., Lamanna, M.C., Ortiz David, L.D., Calvo, J.O., Coria, J.P., 2016. A gigantic new dinosaur from Argentina and the evolution of the sauropod hind foot. Scientific Reports 6, 19165. http://dx.doi.org/10.1038/srep19165.

Green, J.T., Mills, A.M., 2014. Osteogenic tumours of bone. Seminars in Diagnostic Pathology 31, 21–29. http://dx.doi.org/10.1053/j.semdp.2014.01.001.

Greenspan, A., Remagen, W., 2002. Lesiones Vasculares. In: Greenspan, A., Remagen, W. (Eds.), Tumores de Huesos y Articulaciones. Marban Libros S.L, España, pp. 289–310.

Hang, J.F., Chen, P.C.H., 2014. Parosteal Osteosarcoma. Archives of Pathology and Laboratory Medicine 138, 694–699. http://dx.doi.org/10.5858/arpa.2013-0030-RS.

Hanna, R.R., 2002. Multiple injury and infection in a sub-adult theropod dinosaur *Allosaurus fragilis* with comparisons to allosaur pathology in the Cleveland-Lloyd dinosaur Quarry Collection. Journal of Vertebrate Paleontology 22, 76–90. http://dx.doi.org/10.1671/02724634.2002.022.

Hatcher, J.B., 1901. *Diplodocus* Marsh, its osteology, taxonomy and probable habits, with a restoration of the skeleton. Memoirs of the Carnegie Museum 1, 1–64.

Hedrick, B.P., Gao, C., Tumarkin-Deratzian, A.R., Shen, C., Holloway, J.L., Zhang, F., Dodson, P., 2016. An injured *Psittacosaurus* (Dinosauria: Ceratopsia) from the Yixian Formation (Liaoning, China): implications for *Psittacosaurus* biology. The Anatomical Record 299, 897–906. http://dx.doi.org/10.1002/ar. 23363.

Holland, W.J., 1915. Heads and tails: a few notes relating to the structure of the sauropod dinosaurs. Annals of the Carnegie Museum 9, 273–278.

Holliday, C.M., 2009. New insights into dinosaur jaw muscle anatomy. Anatomical Record 292, 1246–1265. http://dx.doi.org/10.1002/ar.20982.

Lambe, L., 1910. Note on the parietal crest of *Centrosaurus apertus*, and a proposed new generic name for *Stereocephalus tutus*. Ottawa Naturalist 24, 149–151.

Lehrer, H.Z., Maxfield, W.S., Nice, C.M., 1970. The periosteal sunburst pattern in metastatic bone. American Journal of Roentgenology 108, 154–161.

López, M.B., 2003. Patología tumoral ósea. In: Llorens, A.I., Morena, A.M. (Eds.), Paleopatología: la enfermedad no escrita. Masson, Barcelona, pp. 249–252.

Lovell, N.C., 1997. Trauma analysis in paleopathology. American Journal of Physical Anthropology 104, 139–170. http://dx.doi.org/10.1002/(SICI)1096-8644(1997)25+<139::AID-AJPA6>3.0.CO;2-#.

Lyman, R.L., 1994. Vertebrate Taphonomy. Cambridge University Press, Cambridge, p. 552.

Mallon, J.C., Ott, C.J., Larson, P.L., Iuliano, E.M., Evans, D.C., 2016. *Spiclypeus shipporum* gen. et sp. nov., a boldly audacious new chasmosaurine ceratopsid (Dinosauria: Ornithischia) from the Judith River Formation (Upper Cretaceous: Campanian) of Montana, USA. PLoS One 11, e0154218. http://dx.doi.org/10.1371/journal.pone.0154218.

Marsh, O.C., 1877. Notice of some new dinosaurian reptiles from the Jurassic Formation. American Journal of Science 14, 514–516.

Marsh, O.C., 1878. Principal characters of American Jurassic dinosaurus. Part 1. American Journal of Science 3, 411–416.

Martinelli, A.G., Teixeira, V.P.A., Marinho, T.M., Fonseca, P.H.M., Cavellani, C.L., Araújo, A.J.G., Ribeiro, L.C.B., Ferraz, L.F.M., 2015. Fused mid-caudal vertebrae in the titanosaur *Uberabatitan ribeiroi* from the Late Cretaceous of Brazil and other bone lesions. Lethaia 48, 456–462. http://dx.doi.org/10.1111/let.12117.

McWhinney, L., Carpenter, K., Rothschild, B.M., 2001a. Dinosaurian humeral periostitis: a case of a juxtacortical lesion in the fossil record. In: Tanke, D.H., Carpenter, K., Skrepnick, M.W. (Eds.), Mesozoic Vertebrate Life. Indiana University Press, Bloomington, pp. 364–377.

McWhinney, L., Rothschild, B.M., Carpenter, K., 2001b. Posttraumatic chronic osteomyelitis in *Stegosaurus* dermal spikes. In: Carpenter, K. (Ed.), The Armored Dinosaurs. Indiana University Press, Bloomington, pp. 141–156.

Meese, M.A., Sebastianelli, W.J., 1996. Periostitis of the upper extremity: a report of 2 cases and literature review. Clinical Orthopaedics and Related Research 324, 222–226.

Miller, T.T., 2008. Bone tumors and tumorlike conditions: analysis with conventional radiography. Radiology 246, 662–674. http://dx.doi.org/10.1148/radiol.2463061038.

Murphey, M.D., Choi, J.J., Kransdorf, M.J., Flemming, D.J., Gannon, F.H., 2000. Imaging of osteochondroma: variants and complications with radiologic pathologic correlation. Radiographics 20, 1407–1434. http://dx.doi.org/10.1148/radiographics.20.5.g00se171407.

Myhrvold, N.P., Currie, P.J., 1997. Supersonic sauropods? tail dynamics in the diplodocids. Paleobiology 23, 393–409.

Norman, D., 1985. The Illustrated Encyclopedia of Dinosaurs. Crescent Books, New York, p. 208.

O'Connor, P.M., 2006. Postcranial pneumaticity: an evaluation of soft tissue influences on the postcranial skeleton and the reconstruction of pulmonary anatomy in archosaurs. Journal of Morphology 267, 1199–1226. http://dx.doi.org/10.1002/jmor.10470.

Ortner, D.J., Putschar, W.G.J., 1981. Identification of Pathological Conditions in Human Skeletal Remains. Smithsonian Institution Press, Washington D.C., p. 488

Osborn, H.F., 1905. *Tyrannosaurus* and other Cretaceous carnivorous dinosaurs. Bulletin of the American Museum of Natural History 21, 259–265.

Otero, A., Vizcaíno, S.F., 2008. Musculatura y función del miembro posterior de *Neuquensaurus australis* (Sauropoda: Titanosauria). Ameghiniana 45, 333–348.

Perez, L., Otero, A., Apesteguía, S., Gallina, P.A., 2009. Estratigrafía y análisis tafonómico de *Bonitasaura salgadoi* Apesteguía, en el sitio «La Bonita» (Cretácico Superior, Río Negro, Argentina). Revista del Museo Argentino de Ciencias Naturales Nueva Serie 11, 39–48.

Petermann, H., Sander, M., 2013. Histological evidence for muscle insertion in extant amniote femora: implications for muscle reconstruction in fossils. Journal of Anatomy 222, 419–436. http://dx.doi.org/10.1111/joa.12028.

Peterson, J.E., Vittore, C.P., 2012. Cranial pathologies in a specimen of *Pachycephalosaurus*. PLoS One 7, e36227. http://dx.doi.org/10.1371/journal.pone.0036227.

Rana, R.S., Wu, J.S., Eisenberg, R.L., 2009. Periosteal reaction. American Journal of Roentgenology 193, W259–W272. http://dx.doi.org/10.2214/AJR.09.3300.

Redelstorff, R., Hayashi, S., Rothschild, B.M., Chinsamy, A., 2015. Non-traumatic bone infection in stegosaurs from Como Bluff, Wyoming. Lethaia 48, 47–55. http://dx.doi.org/10.1111/let.12086.

Rega, E., 2012. Disease in dinosaurs. In: Brett-Surman, M.K., Holtz, T.R.J., Farlow, J.O. (Eds.), The Complete Dinosaur. Indiana University Press, Bloomington, pp. 666–711.

Reid, R.E.H., 1996. Bone histology of the Cleveland-Lloyd dinosaurs and dinosaurs in general, part I: introduction: Introduction to bone tissues. Brigham Young University Geology Studies 41, 25–71.

Resnick, D., 2002. Diagnosis of Bone and Joint Disorders, fourth ed. Saunders, New York, p. 5472.

Rogers, J., Shepstone, L., Dieppe, P., 1997. Bone formers: osteophyte and enthesophyte formation are positively associated. Annals of the Rheumatic Diseases 56, 85–90. http://dx.doi.org/10.1136/ard.56.2.85.

Rothschild, B.M., 1987. Diffuse idiopathic skeletal hyperostosis as reflected in the paleontologic record: dinosaurs and early mammals. Seminars in Arthritis and Rheumatism 27, 119–125.

Rothschild, B.M., 1997. Dinosaurian paleopathology. In: Farlow, J.O., Brett-Surman, M.K. (Eds.), The Complete Dinosaur. University of Indiana Press, Bloomington, pp. 426–448.

Rothschild, B.M., 2009. Scientifically rigorous reptile and amphibian osseous pathology: lessons for forensic herpetology from comparative and paleopathology. Applied Herpetology 6, 47–79. http://dx.doi.org/10.1163/157075409X413842.

Rothschild, B.M., 2010. Macroscopic recognition of non-traumatic osseous pathology in the post-cranial skeletons of crocodilians and lizards. Journal of Herpetology 44, 13–20. http://dx.doi.org/10.1670/08-243.1.

Rothschild, B.M., Berman, D., 1991. Fusion of caudal vertebrae in late Jurassic sauropods. Journal of Vertebrate Paleontology 11, 29–36. http://dx.doi.org/10.1080/02724634.1991.10011373.

Rothschild, B.M., Martin, L.D., 1993. Paleopathology: Disease in the Fossil Record. CRC Press, Boca Raton, p. 386.

Rothschild, B.M., Martin, L.D., 2006. Skeletal impact of disease. New Mexico Museum of Natural History and Science Bulletin 33, 1–226.

Rothschild, B.M., Rothschild, C., 1994. No laughing matter: spondyloarthropathy and osteoarthritis in Hyaenidae. Journal of Zoo and Wildlife Medicine 25, 259–263.

Rothschild, B.M., Tanke, D.H., Hershkovitz, I., Schultz, M., 1998. Mesozoic neoplasia: origins of haemangioma in the Jurassic age. The Lancet 351, 1862. http://dx.doi.org/10.1016/S0140-6736(05)78809-7.

Rothschild, B.M., Witzke, B.J., Hershkovitz, I., 1999. Metastatic cancer in the Jurassic. Lancet 354, 398.

Straight, W.H., Davis, G.L., Skinner, H.C.W., Haims, A., McClennan, B.L., Tanke, D.H., 2009. Bone lesions in hadrosaurs: computed tomographic imaging as a guide for paleohistologic and stable-isotopic analysis. Journal of Vertebrate Paleontology 29, 315–332. http://dx.doi.org/10.1671/039.029.0211.

Sullivan, R.M., Tanke, D.H., Rothschild, B.M., 2000. An impact fracture in an ornithomimid (Ornithomimosauria: Dinosauria) metatarsal from the Upper Cretaceous (Late Campanian) of New Mexico. New Mexico Museum of Natural History Bulletin 17, 109–111.

Tanke, D.H., Rothschild, B.M., 2002. Dinosaurs: An annotated bibliography of dinosaur paleopathology and related topics 1838–2001. New Mexico Museum of Natural History and Science Bulletin 20, 1–97.

Tanke, D.H., Rothschild, B.M., 2014. Paleopathology in Late Cretaceous Hadrosauridae from Alberta, Canada. In: Eberth, D.A., Evans, D.C. (Eds.), Hadrosaurs. Indiana University Press, Bloomington, pp. 540–571.

Tarsitano, S.F., 1981. Pelvic and Hindlimb Musculature of Archosaurian Reptiles (Unpubl. PhD). City University of New York, 191 pp.

Tschopp, E., Wings, O., Frauenfelder, T., Rothschild, B.M., 2016. Pathological phalanges in a camarasaurid sauropod dinosaur and implications on behaviour. Acta Palaeontologica Polonica 61, 125–134. http://dx.doi.org/10.4202/app.00119.2014.

Tsuihiji, T., 2004. The ligament system in the neck of *Rhea americana* and its implication for the bifurcated neural spines of sauropod dinosaurs. Journal of Vertebrate Paleontology 24, 165–172. http://dx.doi.org/10.1671/A1129-12.

Waldron, T., 2009. Palaeopathology. Cambridge University Press, Cambridge, p. 279.

Wenaden, A.E.T., Szyszko, T.A., Saifuddin, A., 2005. Imaging of periosteal reactions associated with focal lesions of bone. Clinical Radiology 60, 439–456. http://dx.doi.org/10.1016/j.crad.2004.08.017.

Weston, D.A., 2012. Nonspecific infection in paleopathology: interpreting periosteal reactions. In: Grauer, A.L. (Ed.), A Companion to Paleopathology. Wiley-Blackwell, Oxford, pp. 492–512.

Wilson, M.V., 1988. Taphonomic processes: information loss and information gain. Geoscience Canada 15, 131–148.

Wilson, J.A., Carrano, M.T., 1999. Titanosaurs and the origin of "wide-gauge" trackways: a biomechanical and systematic perspective on sauropod locomotion. Paleobiology 25, 252–267. http://dx.doi.org/10.1002/9781444345940.ch27.

Witmer, L.M., 1997. The evolution of the antorbital cavity of archosaurs: a study in soft-tissue reconstruction in the fossil record with an analysis of the function of pneumaticity. Journal of Vertebrate Paleontology 17 (S1), 1–76. http://dx.doi.org/10.1080/02724634.1997.10011027.

Witzmann, F., Asbach, P., Remes, K., Hampe, O., Hilger, A., Paulke, A., 2008. Vertebral pathology in an ornithopod dinosaur: a hemivertebra in *Dysalotosaurus lettowvorbecki* from the Jurassic of Tanzania. The Anatomical Record 291, 1149–1155. http://dx.doi.org/10.1002/ar.20734.

Xing, L.D., Dong, H., Peg, Z., Shu, C.K., Hu, X.D., Jiang, H., 2009. A scapular fracture in *Yangchuanosaurus hepingensis* (Dinosauria: Theropoda). Geological Bulletin of China 28, 1390–1395.